

# BMPR2 influences the response of pulmonary microvascular endothelial cells to inflammatory mediators

Leanda Vengethasamy<sup>1</sup> · Aurélie Hautefort<sup>2</sup> · Birger Tielemans<sup>1</sup> · Catharina Belge<sup>3</sup> · Frédéric Perros<sup>2</sup> · Stijn Verleden<sup>1</sup> · Elie Fadel<sup>4</sup> · Dirk Van Raemdonck<sup>5</sup> · Marion Delcroix<sup>3</sup> · Rozenn Quarck<sup>3</sup>

Received: 10 July 2016 / Revised: 13 October 2016 / Accepted: 24 October 2016 / Published online: 6 November 2016  
© Springer-Verlag Berlin Heidelberg 2016

**Abstract** Mutations in the *bone morphogenetic protein receptor (BMPR2)* gene have been observed in 70 % of patients with heritable pulmonary arterial hypertension (HPAH) and in 11–40 % with idiopathic PAH (IPAH). However, carriers of a *BMPR2* mutation have only 20 % risk of developing PAH. Since inflammatory mediators are increased and predict survival in PAH, they could act as a second hit inducing the development of pulmonary hypertension in *BMPR2* mutation carriers. Our specific aim was to determine whether inflammatory mediators could contribute to pulmonary vascular cell dysfunction in PAH patients with and without a *BMPR2* mutation. Pulmonary microvascular endothelial cells (PMEC) and arterial smooth muscle cells (PASMC) were isolated from lung parenchyma of transplanted PAH patients, carriers of a *BMPR2* mutation or not, and from lobectomy patients or lung

donors. The effects of CRP and TNF $\alpha$  on mitogenic activity, adhesiveness capacity, and expression of adhesion molecules were investigated in PMECs and PASMCs. PMECs from *BMPR2* mutation carriers induced an increase in PASMC mitogenic activity; moreover, endothelin-1 secretion by PMECs from carriers was higher than by PMECs from non-carriers. Recruitment of monocytes by PMECs isolated from carriers was higher compared to PMECs from non-carriers and from controls, with an elevated ICAM-1 expression. CRP increased adhesion of monocytes to PMECs in carriers and non-carriers, and TNF $\alpha$  only in carriers. PMEC from *BMPR2* mutation carriers have enhanced adhesiveness for monocytes in response to inflammatory mediators, suggesting that *BMPR2* mutation could generate susceptibility to an inflammatory insult in PAH.

**Keywords** *BMPR2* · Inflammation · Pulmonary arterial hypertension · Endothelial cells · Smooth muscle cells

✉ Rozenn Quarck  
rozenn.quarck@kuleuven.be

- <sup>1</sup> Respiratory Division, Department of Clinical and Experimental Medicine, University of Leuven, Leuven, Belgium
- <sup>2</sup> UMR-S 999, INSERM and Université Paris-Sud, Laboratoire d'Excellence (LabEx) en Recherche sur le Médicament et l'Innovation Thérapeutique (LERMIT), Centre Chirurgical Marie Lannelongue, Le Plessis-Robinson, France
- <sup>3</sup> Respiratory Division, University Hospitals and Department of Clinical and Experimental Medicine, University of Leuven, Leuven, Belgium
- <sup>4</sup> Service de Chirurgie Thoracique, Vasculaire et de Transplantation Cardio-Pulmonaire, Laboratoire de Recherche Chirurgicale, INSERM U999, Centre Chirurgical Marie Lannelongue, Université Paris-Sud, Le Plessis-Robinson, France
- <sup>5</sup> Experimental Thoracic Surgery and Thoracic Surgery Unit, University Hospitals, University of Leuven, Leuven, Belgium

## Introduction

Pulmonary arterial hypertension (PAH) is a severe progressive disease defined hemodynamically by a mean pulmonary arterial pressure (mPAP) higher than 25 mmHg, a pulmonary vascular resistance (PVR) higher than 3 Woods units and a pulmonary artery wedge pressure (PAWP) lower than 15 mmHg. PAH is characterized by a distal pre-capillary arteriopathy, resulting in increased pulmonary vascular resistance, right ventricular hypertrophy, progressive right heart failure, and ultimately death [17, 30]. Idiopathic PAH (IPAH) is sporadic when no familial history or identified risk factor is reported [38]. In patients with a familial history of PAH, germline mutations in the *bone morphogenetic protein receptor type 2 (BMPR2)* gene are detected in 70 % of patients

[42]. However, *BMPR2* gene mutations have also been detected in up to 25 % of apparently idiopathic cases without any familial history [42]. *BMPR2* mutation carriers develop PAH 10 years earlier than non-carriers and have a more severe hemodynamic compromise and a reduced response to vasodilator testing [9, 28, 35]. Bone morphogenetic proteins, members of the TGF- $\beta$  superfamily, bind to BMPRII and are involved in cellular functions including osteogenesis, cell differentiation, growth, and homeostasis [22, 24]. Identification of *BMPR2* mutations in PAH patients has highlighted the relevance of the TGF- $\beta$  superfamily of receptors in the pathophysiology of PAH. Accordingly, bone morphogenetic protein and TGF $\beta$ 1 signalling plays a major role in the pathogenesis of PAH as evidenced by (i) the involvement of downstream effectors of BMP receptor, SMAD proteins [45], and (ii) the identification of mutations in other TGF-beta family receptor members or related downstream signalling proteins, including ALK1, endoglin, and SMAD9 in a small percentage of heritable PAH cases [21, 42]. Among *BMPR2* mutation carriers, only 20 % will later develop PAH, which suggests that a *BMPR2* mutation alone is not sufficient to cause PAH [42]. Interestingly, increased susceptibility to pulmonary hypertension is observed heterozygous null *BMPR2* mice when an additional inflammatory stimulus is applied [39], under hypoxia [1], or infusion of serotonin [19]. More recently, Sawada et al. [37] have shown an increase in the translation of the cytokine granulocyte macrophage colony-stimulating factor (GM-CSF) in *BMPR2* deficient human pulmonary artery endothelial cells (PAEC) following tumour necrosis factor alpha (TNF $\alpha$ ) stimulation. In human PAH, the pathophysiological processes commonly involved are vascular remodelling, vasoconstriction, thrombosis, and inflammation [15]. Vascular remodelling involves pulmonary arterial smooth muscle cell (PASMC) and PAEC proliferation, migration, and mesenchymal transition [25, 34]. In addition, perivascular inflammation may contribute to vascular remodelling [7, 25, 43]. Circulating levels of cytokines including interleukin (IL)-1 $\beta$ , IL-6, and TNF $\alpha$  are increased, and cytokine and chemokine-dependent mechanisms lead to inflammatory cell recruitment in human PAH [10, 13, 33, 36, 40]. It is currently and widely accepted that inflammation and autoimmunity can contribute to PAH pathobiology [4]. More recently, BMPRII deficiency has been shown to increase cytokine production [41]. We have shown that circulating levels of C-reactive protein (CRP), a well-known inflammatory marker, are increased in PAH and can predict adverse outcomes in PAH patients [31]. The effects of CRP at the cellular level have not been studied in PAH.

We determined whether loss of BMPRII signalling could modify basal levels of inflammatory molecule expression and cellular response to circulating inflammatory mediators in PMECs and PASMCs. Therefore, we investigated the effects of the inflammatory mediators TNF $\alpha$  and

CRP on pulmonary vascular cell function in PAH patients with impaired BMPRII signalling.

## Materials and methods

### Materials

Cell culture media including Dulbecco's modified Eagle's medium (DMEM) and RPMI, foetal bovine serum (FBS), penicillin, streptomycin, fungizone, dispase, Hank's balanced salt solution (HBSS), phosphate buffered saline (PBS), 4',6-diamidino-2-phenylindole (DAPI), TRIzol, SuperScript<sup>TM</sup> III First-Strand Synthesis System, primers, RT<sup>2</sup> SYBR Green/ROX qPCR Master Mix, and secondary antibodies conjugated with Alexa Fluor were purchased from Life Technologies. Vascular cell adhesion molecule-1 (VCAM-1) primers were purchased from Integrated DNA Technologies. Pre-designed endothelin converting enzyme-1 (ECE-1) primers were purchased from Bio-Rad. Fibronectin, TNF $\alpha$ , and highly purified, endotoxin-free human recombinant CRP were purchased from R&D Systems. Gelatin and bovine serum albumin (BSA) were purchased from Sigma-Aldrich. [<sup>3</sup>H]-thymidine (specific activity 74 GBq mmol<sup>-1</sup>) was from Perkin Elmer. RNeasy Mini Kit and RNase-Free DNase set were purchased from Qiagen. Anti-human CD31 antibody coupled to allophycocyanin fluorochrome (CD31-APC) was from Miltenyi Biotec. Lab-Tek chamber slides were from Nunc. U937 cells were a gift from the laboratory of clinical immunology (KU Leuven, Belgium). Monoclonal antibodies raised in mouse against human alpha smooth muscle actin ( $\alpha$ -SMA; clone 1A4), human desmin, human CD31 (clone JC70A), and human von Willebrand factor (vWF) (clone F8/86) were purchased from Dako. Polyclonal antibody raised in rabbit against human smooth muscle myosin heavy chain (SMMHC) was from Biomedical Technologies. Acetylated low-density lipoprotein (LDL) coupled to a fluorescent carbocyanine dye, 1,1'-dioctadecyl-3,3',3''-tetramethylindocarbocyanine perchlorate (DiI-Ac-LDL), was purchased from Tebu-Bio. Monoclonal antibodies raised in mouse against human intercellular adhesion molecule-1 (ICAM-1) and VCAM-1 were from R&D Systems and polyclonal antibodies raised in rabbit against peptide comprising amino-acids 950 to C-terminus of human BMPRII were from abcam. Mouse monoclonal antibody against  $\beta$ -actin (clone AC-74) was from Sigma. Secondary antibodies conjugated with horseradish peroxidase were from Jackson.

PMECs were cultured in microvascular endothelial cell growth medium containing 6 % growth supplement, 100 U/mL penicillin, 100  $\mu$ g/mL streptomycin, and 1.25  $\mu$ g/mL fungizone and starved in microvascular endothelial cell medium supplemented with 0.2 % growth supplement. Microvascular PASMC were cultured in DMEM

supplemented with 10 % FBS, 100 U/mL penicillin, 100 µg/mL streptomycin, and 1.25 µg/mL fungizone and starved in DMEM supplemented with 0.2 % FBS, 100 U/mL penicillin, 100 µg/mL streptomycin, and 1.25 µg/mL fungizone. U937 cells were cultured in RPMI containing 10 % FBS, 100 U/mL penicillin, 100 µg/mL streptomycin, and 1.25 µg/mL fungizone.

### Tissue collection and cell isolation

Lung parenchyma was collected at the time of lung transplantation from PAH patients without *BMPR2* mutation (non-carriers;  $n = 7$ ) and PAH patients with *BMPR2* mutation (carriers;  $n = 5$ ). In addition, lung parenchyma was collected from control subjects at the time of lobectomy or pneumonectomy for suspected localized lung tumor ( $n = 3$ ) and from an unused donor lung ( $n = 1$ ). The study protocol was approved by the Institutional Ethics Committee of the University of Leuven and participants gave written informed consent.

To isolate PMEC, a peripheral section of lung parenchyma was cut into 5-mm pieces and enzymatically digested using 2 U/mL dispase in HBSS for 90 min at 37 °C. The sample was vortexed and flushed with a 10-mL pipette at 20-min intervals during digestion. The tissue homogenate was filtered using a 70-µm cell strainer (BD Falcon) and the filtrate was centrifuged for 8 min, at 20 °C, at 500×g. The cell pellet was resuspended and microvascular PMEC were cultured in gelatin-coated (2 mg/mL) 6-well plates in microvascular endothelial cell growth medium containing 6 % growth supplement, 100 U/mL penicillin, 100 µg/mL streptomycin, and 1.25 µg/mL fungizone. When the cells reached 90 % confluence, immunomagnetic purification of PMEC was performed using CD31 monoclonal antibody-labelled microbeads (Miltenyi Biotec) as previously described [47]. Immunomagnetic purification of PMEC was repeated three times at 1-week intervals.

Microvascular pulmonary arteries with a diameter smaller than 500 µm were dissected in the laboratory under a microscope from sections of lung parenchyma. To prevent any contamination by fibroblasts, adventitial tissue was removed from pulmonary arterial sections using forceps. PASMC were isolated using the explant-outgrowth method previously described [32] and cultured in DMEM supplemented with 10 % FBS. All experiments with PMEC and PASMC were carried out with cells which have undergone less than 8 passages.

### Phenotyping of PMEC and PASMC

Primary PMEC were phenotyped as previously described [32]. Briefly, PMEC phenotype was characterized by labelling cells with diI-Ac-LDL and by immunofluorescence using monoclonal antibodies against human CD31 and human

vWF. In addition, CD31 positive, viable PMEC were quantified by fluorescent-activated cell sorting (FACS, FacsCanto II, Becton Dickinson). Cells were incubated with allophycocyanin (APC)-conjugated CD31 antibody (Miltenyi Biotec) for 15 min at 4 °C. Stained cells were washed and at least 10,000 events were measured by FACS. Microvascular PASMCs were phenotyped by immunofluorescence using antibodies raised against  $\alpha$ -SMA, desmin and human SMMHC as previously described [32]. For quantification of immunofluorescence staining, 10 images from non-overlapping fields on each slide were captured at  $\times 40$  magnification. Cells were counted by a single observer, unaware of the identity of each section.

### Cell proliferation

Subconfluent microvascular PASMCs were starved for 96 h in DMEM supplemented with 0.2 % FBS, and PMEC were starved for 24 h in microvascular endothelial cell medium supplemented with 0.2 % growth supplement. Mitogenic activity of PASMC was measured by adding increasing concentrations of FBS or 10 µg/mL CRP and 0.5 µCi/mL of [<sup>3</sup>H]-thymidine (74 GBq/mmol, GE Healthcare) for 48 h. PMEC proliferation was measured by adding increasing concentrations of growth supplement and 0.5 µCi/mL of [<sup>3</sup>H]-thymidine for 18 h. Trichloroacetic acid-insoluble cell material was solubilized in 0.2 N NaOH and radioactivity incorporation was quantified in a  $\beta$ -scintillation liquid counter as previously described [32]. Experiments were performed in triplicate. Data are expressed as fold increase vs. control (0.2 % FBS).

### Co-culture of PMEC and PASMC

PMEC were seeded at a density of 45,000 cells/cm<sup>2</sup> on gelatin-coated Transwell® inserts (12 mm diameter, 0.4 µm pore size, Corning). Confluent PMEC were starved for 24 h in microvascular endothelial cell starving medium. In parallel, subconfluent PASMC were starved in PASMC starving medium for 72 h. Following wash-out with PBS, inserts containing PMEC were placed above PASMC in DMEM-0.2 %FBS containing 0.5 µCi/mL of [<sup>3</sup>H]-thymidine for 48 h as shown in Fig. 1. Radioactivity incorporation was quantified as described above. All experiments were performed in triplicate. Data are expressed as fold increase vs. control (in the absence of PMECs).

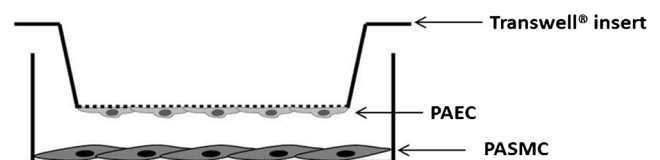


Fig. 1 Diagram of PMECs and PASMCs in co-culture

### PMEC adhesiveness for monocytes

Subconfluent PMECs were starved for 24 h and stimulated with 10 µg/mL CRP or 10 ng/mL TNF $\alpha$  for 3 h. Human monocytic U937 cells in suspension were radio-labelled with 1 µCi [ $^3$ H]-thymidine per 10 $^6$  cells for 48 h and added ( $5 \times 10^5$  per well) to the endothelial cell monolayer for 3 h at 37 °C. Non-adherent cells were washed out. Radioactivity incorporated into monocytes in suspension and attached to the EC monolayer was quantified as previously described [47]. Data are expressed as percentage of adhering cells over cells initially added.

### Adhesion molecule expression and quantification

PMEC seeded onto fibronectin-coated chamber slides were stimulated with 10 µg/mL CRP for 3 h at 37 °C. PMEC were not permeabilized in order to detect only adhesion molecules expressed at the cell surface. ICAM-1 and VCAM-1 expression was detected by immunofluorescence using antibodies against ICAM-1 and VCAM-1 (dilution 1:50). TNF $\alpha$  (10 ng/mL) was used as a positive control. For quantification of immunofluorescence staining, 10 images from non-overlapping fields on each slide were captured at 40 $\times$  magnification. Cells were counted by a single observer, unaware of the identity of each section. PMEC displaying a positive staining at their surface were considered positive for the specific staining and results were expressed as the percentage of cells expressing the cell surface adhesion molecule over total number of cells.

### RNA isolation and reverse transcription

Total RNA was extracted from lung tissue, PMEC and microvascular PASM by a single-step method (TRIzol) based on the guanidium isothiocyanate acid phenol method, followed by on column-based purification using RNeasy mini kit. Genomic DNA was removed by enzymatic digestion with DNase I (Qiagen). RNA integrity and quantity were evaluated using a chip-based nucleic acid separation system (Prokaryote Total RNA 6000 Nano assay) on the Agilent 100 Bioanalyzer (Agilent Technologies). First-strand cDNA was generated from 1 µg total RNA by reverse transcription using SuperScript<sup>TM</sup> III system.

### Quantitative real-time polymerase chain reaction

Expression levels of BMPR2, ICAM-1, VCAM-1, ECE-1, and the housekeeping gene  $\beta$ -actin were determined by quantitative real-time polymerase chain reaction (qRT-PCR). First-strand cDNA was incubated for 2 min at 50 °C, denatured for 10 min at 95 °C, and subjected to 40 amplification cycles alternating between annealing/extension at 60 °C for 1 min

followed by denaturation at 95 °C for 15 s using a thermal cycler (Eco<sup>TM</sup> Real-Time PCR System, Illumina). Relative expression was calculated using the comparative  $\Delta$ Ct method:  $2^{-\Delta C_t}$  (gene of interest-Ct housekeeping gene). Primers used were as follows: BMPR2, forward 5'TGCAGGTTCTCGTG TCTAGG3' and reverse 5'GGTCCCAACAGTCTTCGATT 3'; ICAM-1, forward 5'CGCTGAGCTCCTCTGCTACT3' and reverse 5'TAGGCAACGGGGTCTCTATG3'; VCAM-1, forward 5'AACCTTGACGCTTACAGTGA3' and reverse 5'TGTGTGAAGGAGTTAATTTGATTGG3';  $\beta$ -actin, forward 5'GGACATCCGCAAAGACCTGT3' and reverse 5'CTCAGGAGGAGCAATGATCTTGAT3'.

### Western blotting

Snap-frozen lung tissue samples were homogenized using a tissue homogenizer (Ultra-Turrax T25, Janke & Kunkel) in ice-cold homogenization buffer containing 50 mM Tris, pH 8.0, 10 mM CHAPS (3-[(3-cholamidopropyl)dimethylammonio]-1-propanesulfonate), 2 mM EDTA, 2 mM EGTA, 1 µg/mL leupeptin, and 1 µg/mL antipain (Complete Mini Protease Inhibitor Cocktail, Roche Diagnostics). Homogenates were centrifuged at 4 °C to remove insoluble material and supernatants were collected. Protein concentrations were determined by the Bradford method [2]. Protein lysates were solubilized in Laemmli buffer, and disulphide bridges were reduced in the presence of  $\beta$ -mercaptoethanol for 5 min at 95 °C. Proteins were further separated on a 10 % acrylamide gel by SDS-PAGE. Proteins were transferred to polyvinylidene fluoride (PVDF) filters by electroblotting for 3 h in a transfer buffer containing 25 mM Tris, pH 8.1–8.5, 192 mM glycine, and 20 % methanol. After blocking in Tris-buffered saline (TBS) containing 0.1 % Tween-20 (TBS-Tween) containing 5 % non-fat dry milk for 1 h at room temperature with rocking, the membrane was incubated with rabbit anti-human BMPRII or anti- $\beta$ -actin antibodies overnight at 4 °C in TBS-Tween containing 5 % non-fat dry milk. The membrane was then washed three times for 10 min in TBS-Tween and incubated with a secondary antibody conjugated with horseradish peroxidase, donkey anti-rabbit immunoglobulin (Ig)G for anti-BMPRII, and anti-mouse IgG for anti- $\beta$ -actin in TBS-Tween for 1 h at room temperature. Peroxidase staining was revealed with a chemiluminescence kit (GE Healthcare), imaged with the Proxima 2850T imaging system (Isogen Life Science) and analysed using the software Totallab (Isogen Life Science).

### Endothelin (ET)-1, interleukin (IL)-6, and IL-8 measurement

Confluent PMEC were starved for 24 h. Fresh medium was added and conditioned medium was collected after 18 h. ET-1 levels were measured using an ELISA kit following the manufacturer's instructions (QuantiGlo, R&D

Systems). Briefly, cell supernatants were incubated in microplates coated with a rat monoclonal antibody against ET-1, unbound substances were washed away, and a mouse monoclonal antibody against ET-1 conjugated to horseradish peroxidase was added to each well. Antibody binding was revealed using an enhanced luminol/peroxide substrate solution. Similarly IL-6 and IL-8 levels were measured using an ELISA kit following the manufacturer's instructions (Quantikine, R&D Systems). Briefly, cell supernatants were incubated in microplates coated with a mouse monoclonal antibody against IL-6 or IL-8, unbound substances were washed away, and a rabbit polyclonal antibody against IL-6 or IL-8 conjugated to horseradish peroxidase was added to each well. Antibody binding was revealed using a tetramethylbenzidine/peroxide substrate solution.

### Statistical analysis

Statistical analyses were performed using GraphPad Prism 4.01 (GraphPad Software Inc., La Jolla, California). Differences between two and three groups were analysed using Student *t* test and ANOVA followed by Tukey post hoc test. Two-way ANOVA test was performed followed by Bonferonni post hoc test. Associations between variables were analysed using Pearson's correlation. A value of  $p < 0.05$  was considered statistically significant. All *p*-values are for two-sided tests. Data are expressed as mean  $\pm$  SEM.

## Results

### Patient characteristics and description of *BMPR2* mutations

Patient characteristics at diagnosis and at lung transplantation are listed in Table 1. We did not observe any difference in age, gender, body mass index, 6-min walking distance, circulating CRP levels, mPAP, cardiac output, cardiac index, PVR, total vascular resistance, whereas right atrial pressure, and PAWP were significantly increased in *BMPR2* mutation carriers at diagnosis. *BMPR2* mutation carrier 1 has a nonsense mutation in exon 6 [c.631C > T; p. Arg211X]; *BMPR2* mutation carrier 2 has a missense mutation in exon 7 [c.901 T > C p. Ser301Pro]; *BMPR2* mutation carrier 3 has a missense mutation in exon 3 [c.280 T > G p. Cys94Gly] [20]; *BMPR2* mutation carrier 4 has a deletion of exon 10; *BMPR2* mutation carrier 5 has a truncating mutation in exon 6 [c.782\_783del, p. Ile261serfsX4].

### Microvascular PMEC and PASMC characterization

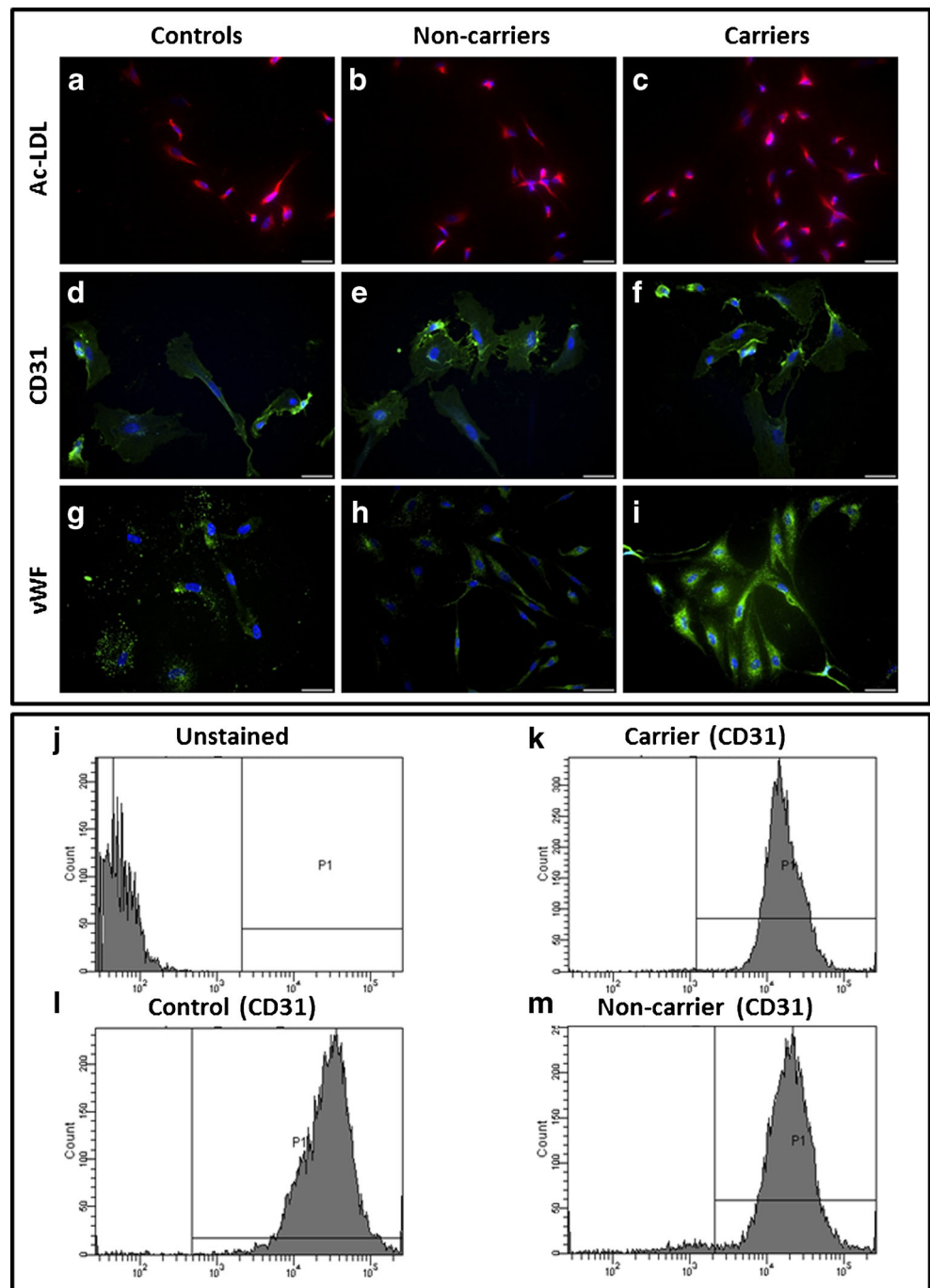
PMECs isolated from controls, non-carriers, and *BMPR2* mutation carriers demonstrated Ac-LDL uptake (Fig. 2a–c), expressed CD31 at their surface (Fig. 2d–f) and contained vWF in Weibel-Palade bodies (Fig. 2g–i). In addition, FACS analysis showed that PMECs expressed CD31 at their surface (Fig. 2j–m). PASMCs isolated from controls, non-carriers, and *BMPR2* mutation carriers

**Table 1** Patient characteristics at diagnosis and lung transplantation

	Diagnosis			Lung Transplantation		
	Non-carriers <i>n</i> = 7	Carriers <i>n</i> = 5	<i>p</i> value (ANOVA, chi-square)	Non-carriers <i>n</i> = 7	Carriers <i>n</i> = 5	<i>p</i> value (ANOVA, chi-square)
Age, years	21 $\pm$ 12	28 $\pm$ 4	0.34	29 $\pm$ 10	43 $\pm$ 8	0.07
Gender, % male	43	40	0.92	43	40	0.92
BMI, kg.m <sup>-2</sup>	23 $\pm$ 5	23 $\pm$ 4	0.93	22 $\pm$ 5	20 $\pm$ 3	0.43
6MWD, m	396 $\pm$ 178	386 $\pm$ 111	0.73	343 $\pm$ 75	403 $\pm$ 115	0.41
CRP, mg.L <sup>-1</sup>	4.8 $\pm$ 4.7	6.3 $\pm$ 3.3	0.57	12.1 $\pm$ 16.7	6.2 $\pm$ 3.6	0.64
RAP, mmHg	5.8 $\pm$ 3.1	11 $\pm$ 4	0.03	11.5 $\pm$ 5.7	10.4 $\pm$ 4.8	0.66
mPAP, mmHg	55 $\pm$ 11	65 $\pm$ 17	0.34	73 $\pm$ 27	53 $\pm$ 2	0.43
PAWP, mmHg	6 $\pm$ 1	13 $\pm$ 5	0.009	11 $\pm$ 6	NA	–
CO, L.min <sup>-1</sup>	4.6 $\pm$ 2.0	4.0 $\pm$ 1.5	0.75	4.7 $\pm$ 2.1	4.6 $\pm$ 2.0	1.00
CI, L min <sup>-1</sup> .m <sup>2</sup>	2.6 $\pm$ 1.0	2.3 $\pm$ 0.8	0.54	2.2 $\pm$ 1.1	2.3 $\pm$ 1.3	0.93
PVR, dyne.s.cm <sup>-5</sup>	1193 $\pm$ 758	1420 $\pm$ 726	0.76	1214 $\pm$ 741	NA	–
TPR, dyne.s.cm <sup>-5</sup>	1273 $\pm$ 806	1529 $\pm$ 842	0.76	1502 $\pm$ 756	1213 $\pm$ 891	0.61

*BMI* body mass index, *6MWD* six-minute walking distance, *CRP* C-reactive protein, *RAP* right atrial pressure, *mPAP* mean pulmonary arterial pressure, *PAWP* pulmonary arterial wedge pressure, *CO* cardiac output, *CI* cardiac index, *PVR* pulmonary vascular resistance, *TPR* total pulmonary resistance

**Fig. 2** PMEC phenotyping. PMECs isolated from pulmonary arteries of controls (**a, d, g**), non-carriers (**b, e, h**), and *BMPR2* mutation carriers (**c, f, i**) were stained with Dil-Ac-LDL (**a–c**) and immuno-labelled with antibodies raised against CD31 (**d–f**) and vWF (**g–i**). Nuclei were counterstained using DAPI (*blue*). CD31 expressed at the surface of PMECs isolated from pulmonary arteries of controls (**l**), non-carriers (**m**), and carriers (**k**) was quantitatively analysed by flow cytometry, compared with unlabelled PMECs (**j**). PMECs were characterized at passage 4. Scale 50  $\mu$ m



displayed  $\alpha$ -SMA filaments and expressed desmin and SMMHC (Fig. 3). Quantitative analysis of the percentage of positive cells is represented in Table 2; more than 80 % of PMECs from controls, non-carriers, and *BMPR2* mutation carriers had Ac-LDL uptake and expressed CD31 and vWF at their surface; moreover, more than 80 % of PASMCs from controls, non-carriers, and *BMPR2* mutation carriers express smooth muscle differentiation markers including  $\alpha$ -SMA, desmin, and SMMHC (Table 2).

### **BMPR2 mRNA and protein expression**

In our settings, we could not detect any significant difference in relative *BMPR2* mRNA expression in lung tissue between *BMPR2* mutation carriers ( $2.43 \pm 0.80$ ), non-carriers ( $3.89 \pm 0.88$ ), and controls ( $3.95 \pm 0.11$ ; ANOVA,  $p = 0.06$ ; Fig. 4a). Similarly, we could not detect any significant difference in *BMPR2* mRNA expression both in PMEC (carriers,  $3.39 \pm 1.41$ , non-carriers,  $2.86 \pm 1.28$ , and controls,  $5.76 \pm 2.24$ ; ANOVA,  $p = 0.09$ ; Fig. 4d), and in PASMC

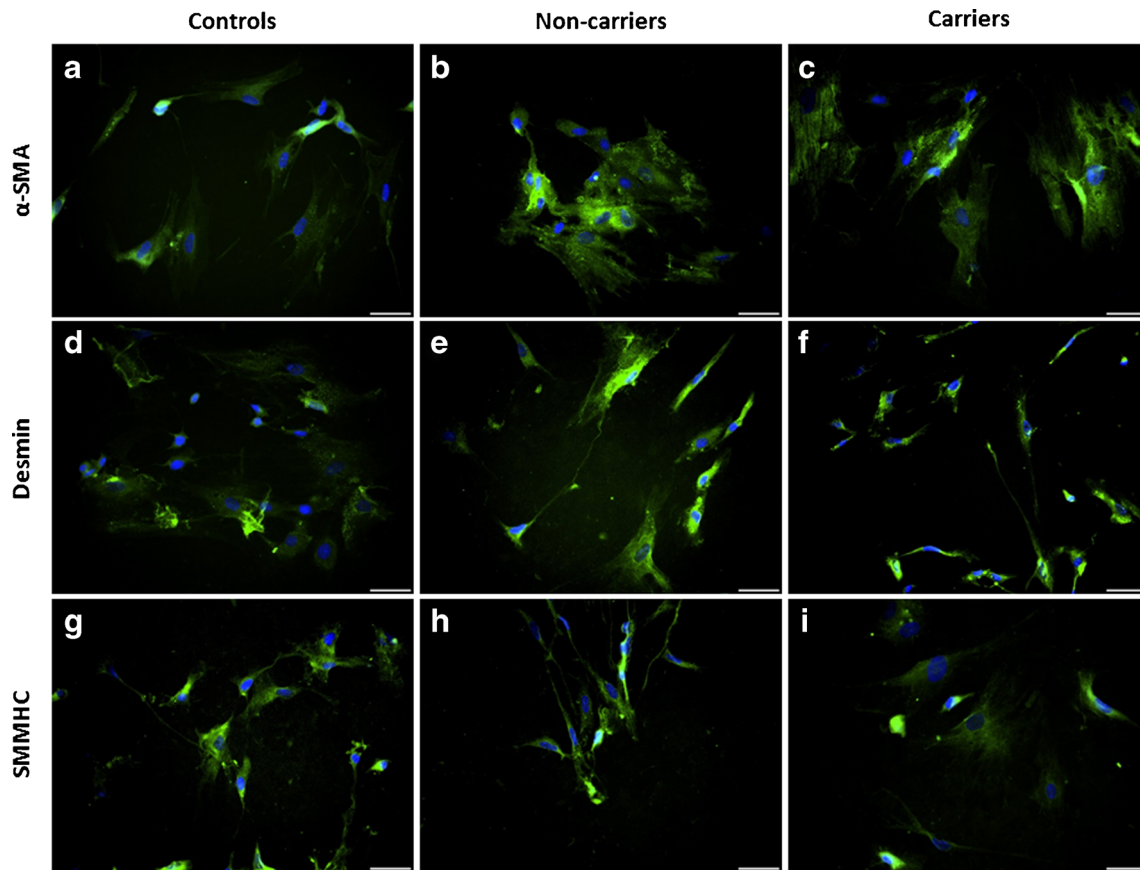


**Fig. 3** PASMCM phenotyping. (a, d, g) PASMCMs isolated from pulmonary arteries of controls, (b, e, h) non-carriers, and (c, f, i) *BMPR2* mutation carriers were immuno-labelled with antibodies raised against  $\alpha$ -SMA

(a–c), desmin (d–f), and SMMHC (g–i). Nuclei were counterstained using DAPI (blue). PASMCMs were characterized at passage 3. Scale 50  $\mu$ m

(carriers,  $0.67 \pm 0.56$ , non-carriers,  $0.54 \pm 0.23$ , and controls,  $1.09 \pm 0.49$ ; ANOVA,  $p = 0.24$ ; Fig. 4c). Moreover, relative protein expression of BMPRII in the lung tissue was not statistically different in *BMPR2* mutation carriers ( $4.20 \pm 1.94$ )

and in non-carriers ( $5.22 \pm 0.23$ ) versus controls ( $7.07 \pm 1.76$ ;  $p = 0.30$ ; Fig. 4b).

**Table 2** PMEC and PASMCM characterization

	Controls (%)	Non-carriers (%)	Carriers (%)
<b>PMECs</b>			
Ac-LDL	$94.7 \pm 5.5$	$91.3 \pm 2.5$	$93.3 \pm 0.6$
CD31	$82.7 \pm 6.0$	$91.7 \pm 2.5$	$88.0 \pm 7.0$
CD31 (FACS)	$98.4 \pm 0.8$	$97.1 \pm 2.1$	$98.7 \pm 1.2$
vWF	$89.3 \pm 2.5$	$86.3 \pm 7.4$	$85.7 \pm 5.6$
<b>PASMCMs</b>			
$\alpha$ -SMA	$86.3 \pm 3.1$	$90.0 \pm 5.0$	$87.7 \pm 2.1$
Desmin	$86.0 \pm 5.6$	$80.6 \pm 13.3$	$88.7 \pm 3.1$
SMMHC	$83.0 \pm 6.6$	$82.0 \pm 13.0$	$87.7 \pm 4.0$

Results are expressed as percentage of alive cells

Ac-LDL acetylated-LDL, vWF von Willebrand factor,  $\alpha$ -SMA  $\alpha$ -smooth muscle actin, SMMHC smooth muscle myosin heavy chain, PMEC pulmonary microvascular endothelial cells, PASMCM pulmonary arterial smooth muscle cells

### PASMCM proliferative properties

Mitogenic activity of PASMCM in response to 5 % FBS appeared higher in *BMPR2* mutation carriers ( $4.1 \pm 3.2$ -fold) compared with non-carriers ( $2.7 \pm 1.5$ -fold) and controls ( $2.0 \pm 0.6$ -fold) ( $p = 0.14$ ; Fig. 5).

Using a co-culture approach, resting PMEC induced PASMCM mitogenic activity to a greater extent in *BMPR2* mutation carriers ( $4.9 \pm 1.0$ -fold increase) than in non-carriers ( $2.8 \pm 0.4$ -fold,  $p < 0.05$ ) and controls ( $2.6 \pm 0.2$ -fold,  $p < 0.05$ ), (Fig. 6a). In addition, cross-over co-culture experiments showed that PMECs isolated from carriers induced enhanced mitogenic activity of PASMCMs isolated from non-carriers ( $1.5 \pm 0.17$ -fold,  $p < 0.01$ ), while PMECs isolated from non-carriers did not induce mitogenic activity of PASMCMs isolated from carriers ( $1.2 \pm 0.32$ -fold,  $p = 0.32$ ) (Fig. 6b). These data suggest that PMECs from *BMPR2* mutation carriers have an enhanced proliferative effect on PASMCMs, potentially driven by altered BMPRII signalling and/or downstream effectors; this could be attributed to

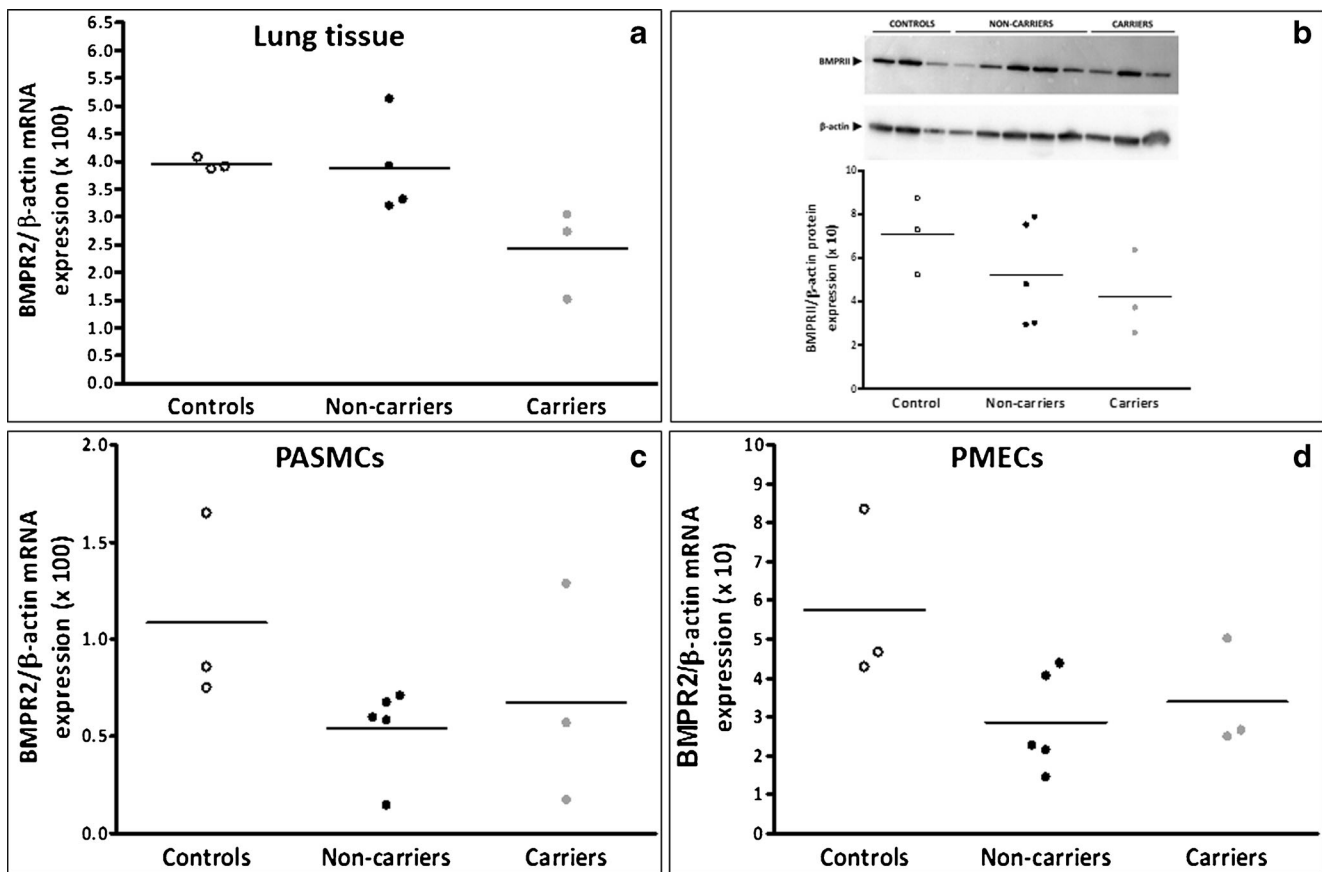


**Fig. 4** *BMPR2* expression. *BMPR2* mRNA expression (a) in lung tissue (ANOVA,  $p = 0.06$ ), (d) PMECs (ANOVA,  $p = 0.09$ ) and (c) PASMCs (ANOVA,  $p = 0.33$ ). (b) Representative image of BMPRII and  $\beta$ -actin

protein expression by Western blotting and quantitative BMPRII protein expression in lung tissue (ANOVA,  $p = 0.30$ )

enhanced ET-1 secretion, as ET-1 secretion by PMEC is significantly higher (ANOVA,  $p = 0.01$ ) in *BMPR2* mutation carriers ( $162 \pm 34$  pg/mL) compared with non-carriers ( $66 \pm 16$  pg/mL) and controls ( $33 \pm 9$  pg/mL) (Fig. 6c). Interestingly, PMEC-induced PASMC mitogenic activity

was correlated with ET-1 levels secreted by PMECs ( $r = 0.76$ ,  $p = 0.04$ ). However, we did not observe any significant difference in the levels of mRNA coding for endothelin converting enzyme-1 (ECE-1), which hydrolyses big endothelin into ET-1, between PMEC from *BMPR2* mutation carriers ( $22.9 \pm 14.1$ ), non-carriers ( $3.9 \pm 1.1$ ) and controls ( $7.1 \pm 3.6$ ). Moreover, we did not find any correlation between individual values of secreted ET-1 and ECE-1 mRNA expression.

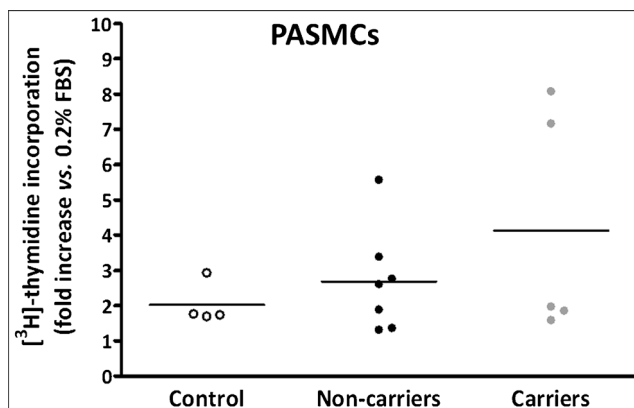


**Fig. 5** PASMC proliferative capacities. Mitogenic activity of PASMCs isolated from controls ( $n = 4$ ), non-carriers ( $n = 7$ ), and *BMPR2* mutation carriers ( $n = 5$ ) in response to 5 % FBS (ANOVA,  $p = 0.31$ ). Independent experiments were performed in triplicate between passages 3 and 5. Data are shown as fold increase vs. 0.2 % FBS

#### PMEC adhesiveness for monocytes and proliferative properties

PMEC mitogenic activity in response to 5 % FBS was similar in controls, non-carriers, and *BMPR2* mutation carriers ( $1.5 \pm 0.2$ -,  $2.0 \pm 0.2$ -,  $1.8 \pm 0.3$ -fold increase, respectively).

Basal adhesiveness of human monocytic cells (U937) to resting PMECs was significantly higher in non-carriers ( $10 \pm 2$  %,  $p < 0.05$ ) and *BMPR2* mutation carriers ( $10 \pm 2$  %,  $p < 0.05$ ), compared with controls ( $2 \pm 0.3$  %) (Fig. 7a). Interestingly, *ICAM-1* mRNA expression was significantly higher in resting PMECs from carriers compared



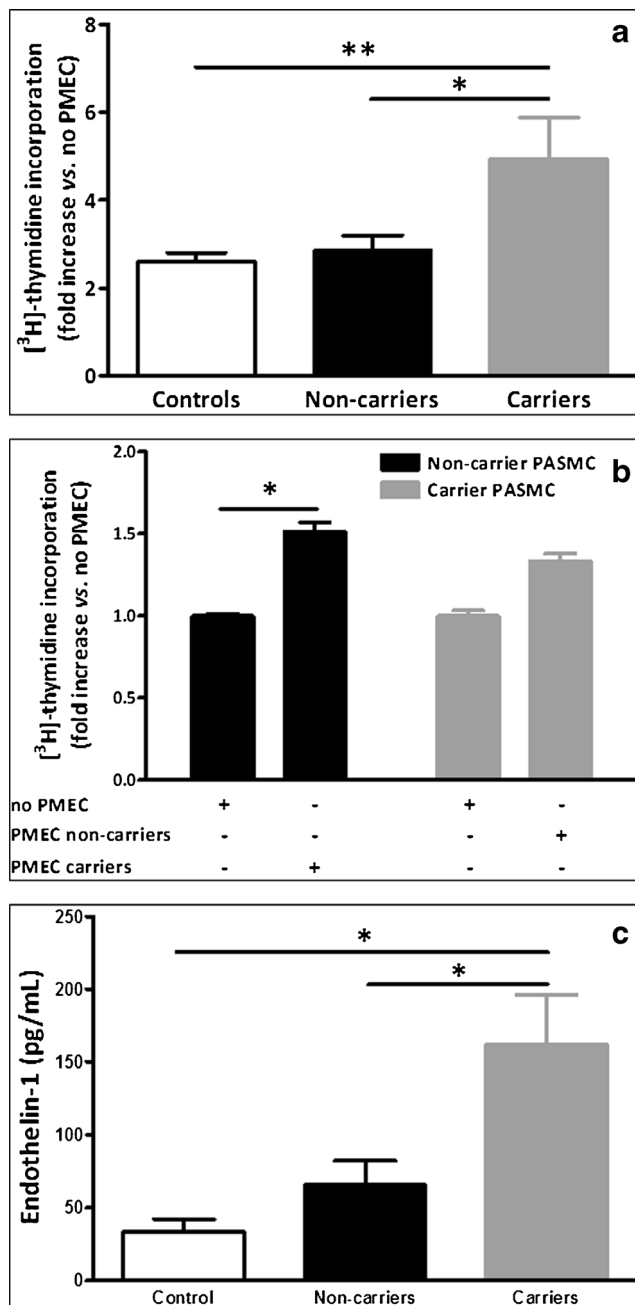


**Fig. 6** Co-culture of PMECs and PSMCs. (a) Mitogenic activity of PSMCs in co-culture with resting PMEC (ANOVA,  $p = 0.02$ ;  $**p < 0.05$ ,  $*p < 0.05$ ). (b) Mitogenic activity of PSMCs from a non-carriers ( $n = 3$ ) and *BMPR2* mutation carriers ( $n = 3$ ) in cross co-culture with resting PMEC from non-carriers ( $n = 3$ ) and *BMPR2* mutation carriers ( $n = 3$ ) (ANOVA,  $p = 0.04$ ;  $*p < 0.01$  vs. 0.2 % FBS). (c) ET-1 secretion by resting PSMCs (ANOVA,  $p = 0.01$ ;  $*p < 0.05$ ). Independent experiments were performed in triplicate between passages 3 and 5. Mitogenic activity data are shown as fold increase vs. 0.2 % FBS

with controls ( $p < 0.05$ ) (Table 3). In addition, ICAM-1 expression appeared increased at the surface of PSMCs from carriers and to a lesser extent from non-carriers (ANOVA,  $p = 0.09$ ; Fig. 7h). VCAM-1 expression was significantly increased at the surface of carrier PSMCs compared with

controls and non-carriers (ANOVA,  $p < 0.05$ ) (Fig. 7i, Table 4), whereas *VCAM-1* mRNA expression was similar in controls, non-carriers and *BMPR2* mutation carriers (Table 3).

#### Effects of an inflammatory trigger on PSMCs and PSMCs

CRP-induced PSMC mitogenic activity was similar in *BMPR2* mutation carriers ( $1.9 \pm 0.7$ -fold), non-carriers ( $1.5 \pm 0.7$ -fold) and controls ( $1.1 \pm 0.6$ -fold) (ANOVA,  $p = 0.23$ ).

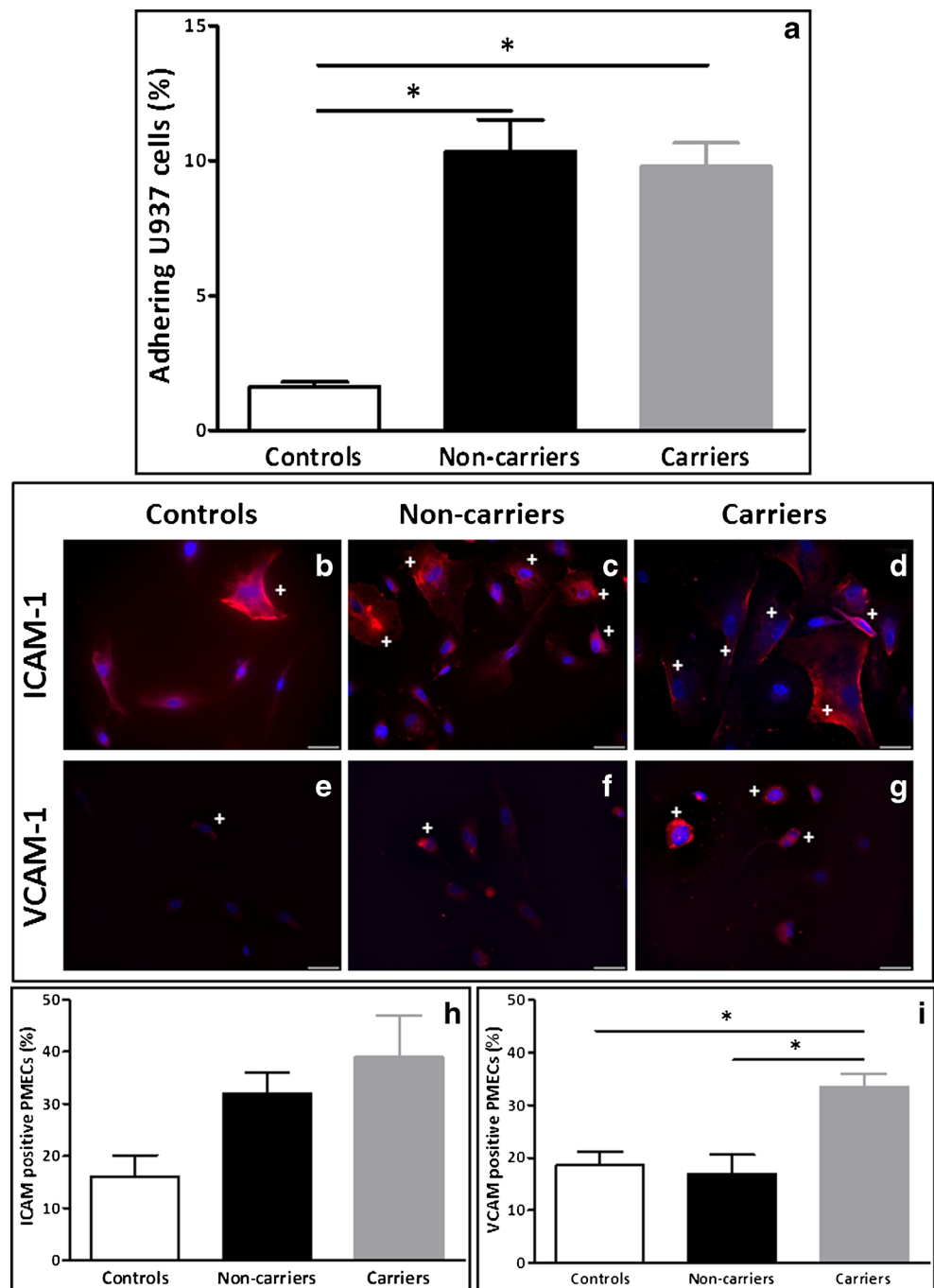
Adhesiveness of U937 cells to  $\text{TNF}\alpha$ -activated PSMC was significantly higher in *BMPR2* mutation carriers ( $50 \pm 6$  %,  $p < 0.05$ ) compared with controls ( $26 \pm 7$  %) (Fig. 8a). In response to CRP, adhesiveness capacity was significantly higher in PAH patients (carriers,  $15 \pm 0.6$  %,  $p < 0.001$  and non-carriers,  $9 \pm 1.6$  %,  $p < 0.05$ ) than in controls ( $2 \pm 0.3$  %) (Fig. 8b).

*ICAM-1* mRNA expression was significantly elevated in PSMCs from *BMPR2* mutation carriers, compared to non-carriers and controls, stimulated by CRP ( $p = 0.011$ ); however, CRP did not induce any increase in *ICAM-1* mRNA expression in PSMCs from *BMPR2* mutation carriers, non-carriers, or controls (Table 3). CRP had no effect on *VCAM-1* mRNA expression in PSMCs from *BMPR2* mutation carriers, non-carriers, or controls (Table 3). CRP had limited effect on ICAM-1 protein expression at the surface of PSMCs from non-carriers and *BMPR2* mutation carriers, whereas it induced ICAM-1 expression in PSMCs from controls (Table 4, Fig. 9).

$\text{TNF}\alpha$  significantly increased *ICAM-1* mRNA expression in PSMCs from controls, *BMPR2* mutation carriers, and non-carriers ( $p < 0.0001$ ) and to a greater extent in PSMCs from *BMPR2* mutation carriers and non-carriers (ANOVA,  $p = 0.06$ ; Table 3).  $\text{TNF}\alpha$  also significantly increased *VCAM-1* mRNA expression in PSMCs from controls, *BMPR2* mutation carriers and non-carriers ( $p < 0.0001$ ); surprisingly,  $\text{TNF}\alpha$ -induced *VCAM-1* mRNA expression was lower in PSMCs from carriers compared with PSMCs from controls ( $p < 0.05$ ; Table 3).  $\text{TNF}\alpha$  increased ICAM-1 expression at the surface of PSMCs from controls, non-carriers, and *BMPR2* mutation carriers, with an enhanced effect on PSMCs from *BMPR2* mutation carriers (Table 4, Fig. 9). In addition,  $\text{TNF}\alpha$  induced increased VCAM-1 expression in PSMCs from non-carriers and *BMPR2* mutation carriers, with an enhanced effect in PSMCs from *BMPR2* mutation carriers (Table 4, Fig. 9).

$\text{TNF}\alpha$  and CRP significantly induced IL-6 production by PSMCs from *BMPR2* mutation carriers but had no effects on IL-8 production (Fig. 10).

**Fig. 7** PMEC adhesiveness to monocytes. **(a)** Adhesiveness of PMECs isolated from controls ( $n = 3$ ), non-carriers ( $n = 5$ ) and *BMPR2* mutation carriers ( $n = 3$ ) to the monocytic cell line U937 at baseline (ANOVA,  $p = 0.04$ ;  $*p < 0.05$ ). Data are shown as percentage of adhering U937 cells. Surface expression of ICAM-1 **(b–d)** and VCAM-1 **(e–g)** in PMECs from controls **(b, e)**, non-carriers **(c, f)** and carriers **(d, g)**. **(h)** Percentage of PMECs expressing ICAM-1 (ANOVA,  $p = 0.09$ ). **(i)** Percentage of PMECs expressing VCAM-1 (ANOVA,  $p = 0.03$ ;  $*p < 0.05$ ). Experiments were performed in triplicate for PMECs from each patient between passages 4 and 7



## Discussion

In the present study, we showed that compared with PMECs from non-carriers, PMECs from *BMPR2* mutation carriers have increased adhesiveness to monocytes, enhanced by CRP and TNF $\alpha$ . Moreover, PMECs from *BMPR2* mutation carriers enhanced PASMC mitogenic activity in co-culture and secreted higher levels of ET-1, a potent pulmonary vasoconstrictor and one of the main therapeutic target in PAH. These observations suggest a dysfunction of PMECs in

*BMPR2* mutation carriers, potentially enhanced by inflammatory mediators such as CRP or TNF $\alpha$ .

## Effects of *BMPR2* mutations on pulmonary vascular function

In our settings, BMPRII protein expression was not different between *BMPR2* mutation carriers and non-carriers. The current 300 listed *BMPR2* mutations include missense and nonsense mutations; whereas nonsense mutations result mostly in

**Table 3** Adhesion molecules mRNA expression in PMECs

Resting	Controls	Non-carriers	Carriers	ANOVA, <i>p</i> value
ICAM-1	$1.5 \times 10^{-3} \pm 0.3 \times 10^{-3}$	$5.6 \times 10^{-3} \pm 2.9 \times 10^{-3}$	$12.3 \times 10^{-3} \pm 2.8 \times 10^{-3}\#$	<b>0.018</b>
VCAM-1	$6.3 \times 10^{-4} \pm 1.2 \times 10^{-4}$	$2.2 \times 10^{-4} \pm 1.5 \times 10^{-4}$	$8.5 \times 10^{-4} \pm 5.2 \times 10^{-4}$	0.39
+ CRP	Controls	Non-carriers	Carriers	ANOVA, <i>p</i> value
ICAM-1	$1.5 \times 10^{-3} \pm 0.3 \times 10^{-3}$	$4.2 \times 10^{-3} \pm 2.3 \times 10^{-3}$	$8.0 \times 10^{-3} \pm 2.8 \times 10^{-3}\#$	<b>0.011</b>
VCAM-1	$5.0 \times 10^{-4} \pm 1.2 \times 10^{-4}$	$2.0 \times 10^{-4} \pm 1.1 \times 10^{-4}$	$4.6 \times 10^{-4} \pm 2.3 \times 10^{-4}$	0.40
+ TNF $\alpha$	Controls	Non-carriers	Carriers	ANOVA, <i>p</i> value
ICAM-1	$0.11 \pm 0.01^{\S}$	$0.25 \pm 0.06^{\S}$	$0.24 \pm 0.05^{\S}$	<b>0.06</b>
VCAM-1	$0.17 \pm 0.03^{\S}$	$0.09 \pm 0.03^{\#}$	$0.04 \pm 0.02^{*\S}$	<b>0.02</b>
ANOVA, <i>p</i> value	<b>&lt;0.0001</b>	<b>&lt;0.0001</b>	<b>&lt;0.0001</b>	
ICAM-1				
ANOVA, <i>p</i> value	<b>&lt;0.0001</b>	<b>0.002</b>	<b>0.005</b>	
VCAM-1				

Experiments were performed in triplicate for PMECs from each patient between passages 4 and 7

CRP C-reactive protein, ICAM-1 intercellular adhesion molecule-1, TNF $\alpha$  tumour necrosis factor  $\alpha$ , VCAM-1 vascular cell adhesion molecule-1

\**p* < 0.05 vs. controls;  $\S$  *p* < 0.001 vs. resting; # *p* < 0.01 vs. resting;  $\S$  *p* < 0.05 vs. resting

truncated protein, missense mutations may have no consequence on the protein size but can result in a loss of protein function. Serum-induced PASMCMitogenic activity was not higher in *BMPR2* mutation carriers compared with controls and non-carriers, in agreement with previous studies [5, 26], although in contrast with the findings by Dewachter et al. [6]. However, the high variability in the in vitro mitogenic response of PASMCMitogenic activity could be attributed to the type of *BMPR2*

mutation since the two highest mitogenic responses were found in PASMCMitogenic activity isolated from carriers of entire exon deletion, i.e., exons 2 and 3, and exon 10, whereas the two lowest were observed in carriers of missense mutations and the intermediate one in carrier of a nonsense mutation. This suggests that PASMCMitogenic activity capacities can be driven by the type of *BMPR2* mutation.

In addition, when co-cultured, resting PMECs increased PASMCMitogenic activity in controls, non-carriers and, to a greater extent, in PASMCMitogenic activity isolated from *BMPR2* mutation carriers. Intriguingly, PMECs from *BMPR2* mutation carriers also increased the mitogenic activity of PASMCMitogenic activity from non-carriers. These effects could be attributed to increased secretion of ET-1, a potent PASMCMitogenic activity, by PMECs from *BMPR2* mutation carriers (Fig. 5b), in agreement with previous studies showing increased ET-1 secretion in PMECs from *BMPR2* mutation carriers and *BMPR2* knocked-down PMECs [8, 44]. However, the increase in ET-1 secretion by PMECs from *BMPR2* mutation carriers does not appear to be linked to any change in ECE-1 expression. Interestingly, we found a correlation between ET-1 secretion by PMECs and PMEC-induced PASMCMitogenic activity, suggesting that ET-1 could mediate enhanced effects of PMECs of *BMPR2* mutation carriers on PASMCMitogenic activity.

Moreover, we showed a higher adhesiveness of resting PMECs from non-carriers and *BMPR2* mutation carriers for monocytes which could be attributed to increased *ICAM-1* mRNA expression and *ICAM-1* and *VCAM-1* protein expression at cell surface. This is in agreement with a previous observation of enhanced *ICAM-1* and *VCAM-1* expression in *BMPR2*-knockdown human umbilical vein endothelial cells [16] and increased leukocyte recruitment by *BMPR2*-

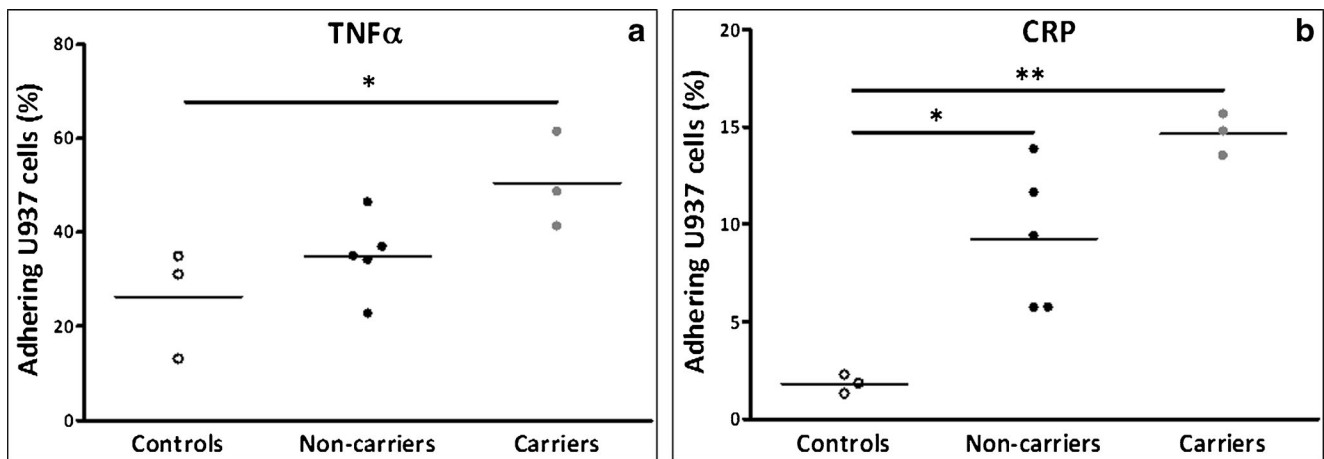
**Table 4** Adhesion molecule expression at PMEC surface

Resting	Controls	Non-carriers	Carriers	ANOVA, <i>p</i> value
ICAM-1	16 $\pm$ 4	32 $\pm$ 4	39 $\pm$ 8	<b>0.09</b>
VCAM-1	19 $\pm$ 2	17 $\pm$ 4	34 $\pm$ 2* $\#$	<b>0.03</b>
+ CRP	Controls	Non-carriers	Carriers	ANOVA, <i>p</i> value
ICAM-1	32 $\pm$ 5 $\S$	35 $\pm$ 9	43 $\pm$ 5	0.57
VCAM-1	26 $\pm$ 4	27 $\pm$ 6	35 $\pm$ 7	0.53
+ TNF $\alpha$	Controls	Non-carriers	Carriers	ANOVA, <i>p</i> value
ICAM-1	43 $\pm$ 3 $\S$	47 $\pm$ 7	62 $\pm$ 4	<b>0.07</b>
VCAM-1	25 $\pm$ 3	38 $\pm$ 5 $\S$	49 $\pm$ 5*	<b>0.04</b>
ANOVA, <i>p</i> value	<b>0.008</b>	0.22	<b>0.07</b>	
ICAM-1				
ANOVA, <i>p</i> value	0.28	<b>0.02</b>	0.18	
VCAM-1				

Experiments were performed in triplicate for PMECs from each patient between passages 5 and 7

CRP C-reactive protein, ICAM-1 intercellular adhesion molecule-1, TNF $\alpha$  tumour necrosis factor  $\alpha$ , VCAM-1 vascular cell adhesion molecule -1

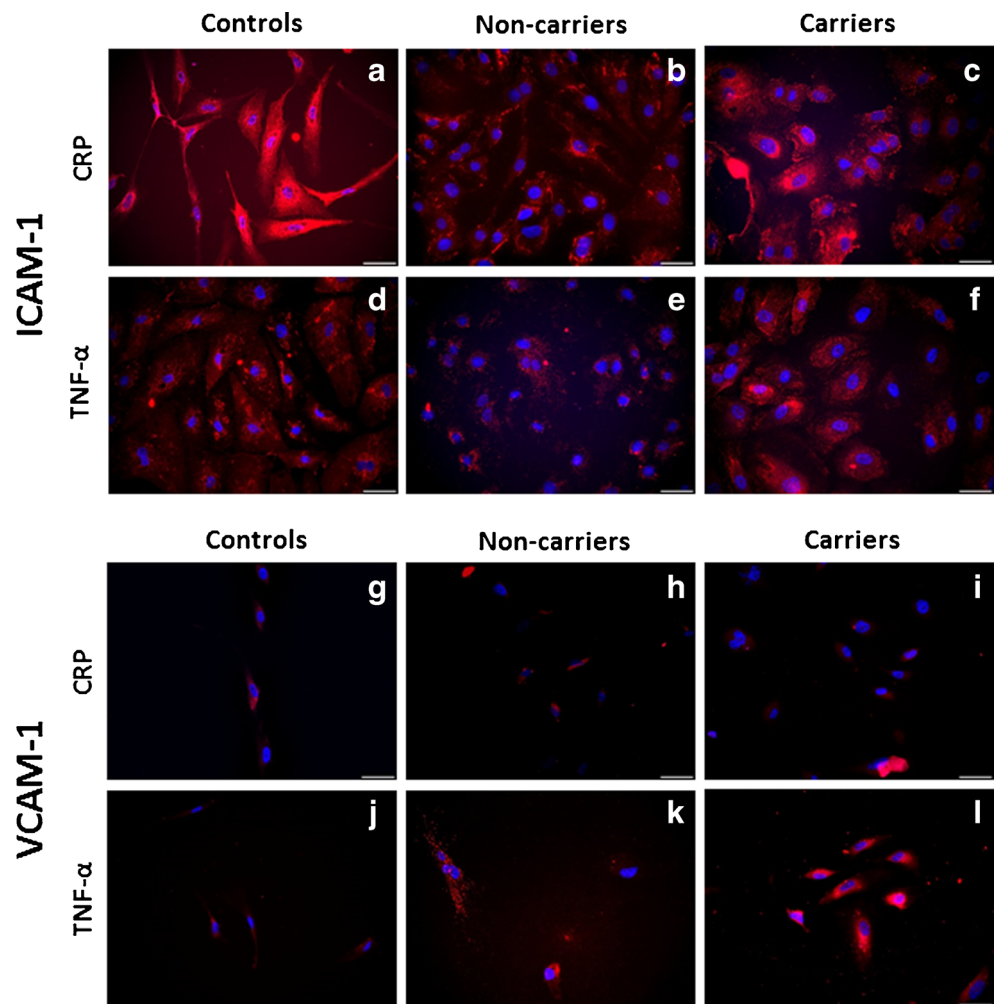
\**p* < 0.05 vs. controls; # *p* < 0.05 vs. non-carriers;  $\S$  *p* < 0.05 vs. resting. Results are expressed as percentage of alive cells



**Fig. 8** Effects of inflammatory mediators on PMEC adhesiveness for monocytes. Adhesiveness capacity of PMECs isolated from controls ( $n = 3$ ), non-carriers ( $n = 5$ ), and *BMP2* mutation carriers ( $n = 3$ ) to the monocytic cell line U937 in response to (a) TNF $\alpha$  (10 ng/ml);

ANOVA,  $p = 0.04$ ; \* $p < 0.05$  and (b) CRP (10  $\mu\text{g/ml}$ ); ANOVA,  $p = 0.001$ , \* $p < 0.05$ , and \*\* $p < 0.001$ . Data are shown as percentage of adhering U937 cells. Experiments were performed in triplicate for PMECs from each patient between passages 4 and 7

**Fig. 9** Effects of inflammatory mediators on adhesion molecule expression at PMEC surface. Expression at surface of PMECs from controls (a, d, g, j), non-carriers (b, e, h, k), and *BMP2* mutation carriers (c, f, i, l) of ICAM-1 (a-f) and VCAM-1 (g-l), after a 3-h stimulation with CRP (a-c, g-i) or TNF $\alpha$  (d-f, j-l). Experiments were performed with PMECs from each patient between passages 5 and 7. Scale 100  $\mu\text{m}$



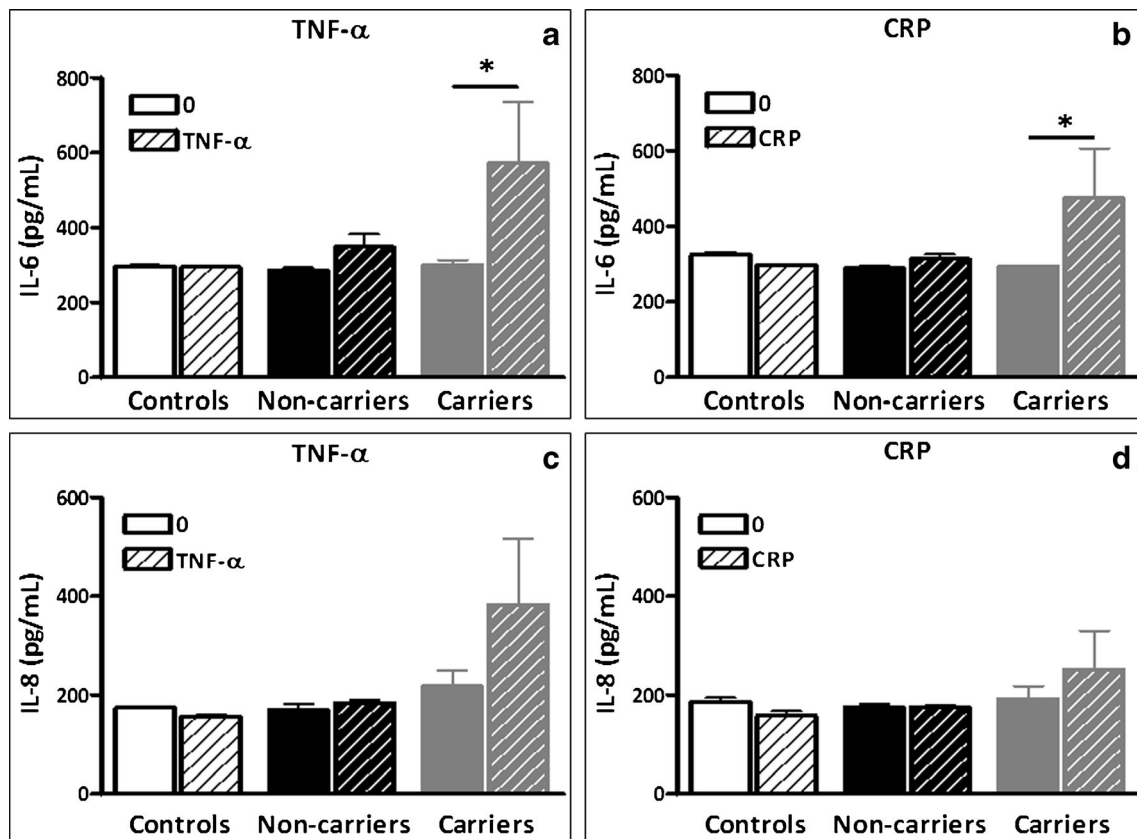


**Fig. 10** Effects of inflammatory mediators on IL-6 and IL-8 secretion by PMECs. Secretion of IL-6 (a, b) and IL-8 (c, d) in the presence of TNF $\alpha$  (a, c) or CRP (b, d) by PMECs isolated from controls ( $n = 3$ ), non-carriers

( $n = 3$ ) and *BMPR2* mutation carriers ( $n = 3$ ). Experiments were performed with PMECs between passages 5 and 7. (a) ANOVA,  $p = 0.03$ ;  $*p < 0.05$ . (b) ANOVA,  $p = 0.05$ ;  $*p < 0.05$

knockdown human PMEC [3]. Interestingly, *BMPR2* genetic ablation in mouse pulmonary endothelium resulted in perivascular leukocyte infiltration, in situ thrombosis and predisposition to PAH [12]. Finally, various functional changes were observed in the pulmonary endothelium in association with BMPRII dysfunction, including apoptosis [46], DNA damage [18] and pulmonary endothelial barrier dysfunction [29].

#### Effects on inflammatory triggers on pulmonary microvascular endothelial cells

Considering the low penetrance of a *BMPR2* mutation, a “second hit” may be required for the development of PAH, in addition to a *BMPR2* mutation [23, 27]. Increased inflammatory mediators, such as circulating CRP and interleukins, have been observed in PAH and were shown to predict survival [31, 40]. Consequently, we hypothesized that inflammatory mediators could contribute to endothelial dysfunction in PAH. We found that CRP and TNF $\alpha$  increased adhesiveness of U937 monocytic cells to PMEC from *BMPR2* mutation carriers, suggesting that BMPRII protein dysfunction could enhance the response of endothelium to inflammatory mediators. In *BMPR2* mutation carriers, CRP-mediated adhesiveness of PMECs for monocytes could be attributed to a

moderate expression of ICAM-1 at the surface of PMECs, whereas TNF $\alpha$ -mediated adhesiveness of PMECs for monocytes could be due to enhanced *VCAM-1* mRNA expression and protein expression at the surface of PMECs. In non-carriers, CRP-mediated adhesiveness could be due to *VCAM-1* expression at the surface of PMECs and TNF $\alpha$ -mediated adhesiveness to enhanced *VCAM-1* mRNA expression and to expression of both ICAM-1 and *VCAM-1* at the surface of PMECs. Moreover, we observed that both TNF $\alpha$  and CRP induced the production of IL-6 by PMECs from *BMPR2* mutation carriers, in agreement with previous studies demonstrating increased levels of circulating IL-6, shown to predict outcome and impaired survival in PAH [11, 14, 40]. Our findings are also in agreement with recent observations showing that (i) mice carrying a mutant *BMPR2* allele lacking exons 4 and 5 harboured mild pulmonary hypertension and impaired pulmonary vascular remodelling under hypoxia [1], (ii) acute exposure to LPS of *BMPR2*<sup>+/-</sup> mice resulted in enhanced production of inflammatory mediators such as IL-6 and KC/IL-8 [39], (iii) pulmonary artery SMC from *BMPR2*<sup>+/-</sup> mice and patients with *BMPR2* mutations produced induced secretion of IL-6 and KC/IL-8 [39], and (iv) rats expressing a *BMPR2* mutant harbour remodelling of distal pulmonary arteries [34].

## Limitations

As pulmonary vascular cells were isolated at the time of lung transplantation, the results from the present study may reflect advanced stages of the disease rather than early pathogenesis. In addition, the low number of patients included could be seen as a constraint; one should highlight that i) IPAH and HPAH are rare diseases and ii) only a very low percentage of patients can benefit from lung transplantation, thus limiting access to human tissue. Regarding the potential crosstalk between PMECs and PASMCs in a context of mutated *BMPR2* gene, it would be relevant to further investigate the effects of ET-1 receptor antagonists.

## Conclusion

We report that inflammatory mediators may contribute to pulmonary microvascular endothelial cell dysfunction in *BMPR2* mutation carriers with PAH. Since *BMPR2* mutation carriers have increased pulmonary vascular cell mitogenic activity and in vitro CRP-induced adhesiveness of PMECs for monocytes, we suggest that *BMPR2* mutations may increase susceptibility of the pulmonary endothelium to adverse effects of inflammatory mediators.

**Acknowledgments** MD is holder of the Actelion chair for Pulmonary Hypertension at the University of Leuven. The authors would like to thank Jennifer Arthur-Ataam for her help in isolating pulmonary vascular cells.

## References

1. Beppu H, Ichinose F, Kawai N, Jones RC, Yu PB, Zapol WM, Miyazono K, Li E, Bloch KD (2004) *BMPR-II* heterozygous mice have mild pulmonary hypertension and an impaired pulmonary vascular remodeling response to prolonged hypoxia. *Am J Physiol Lung Cell Mol Physiol* 287:L1241
2. Bradford MM (1976) A rapid and sensitive method for the quantitation of microgram quantities of protein utilizing the principle of protein-dye binding. *Anal Biochem* 72:248–254
3. Burton VJ, Ciuculan LI, Holmes AM, Rodman DM, Walker C, Budd DC (2011) Bone morphogenetic protein receptor II regulates pulmonary artery endothelial cell barrier function. *Blood* 117:333–341
4. Cohen-Kaminsky S, Hautefort A, Price L, Humbert M, Perros F (2014) Inflammation in pulmonary hypertension: what we know and what we could logically and safely target first. *Drug Discov Today* 19:1251–1256
5. Davies RJ, Holmes AM, Deighton J, Long L, Yang X, Barker L, Walker C, Budd DC, Upton PD, Morrell NW (2012) BMP type II receptor deficiency confers resistance to growth inhibition by TGF-beta in pulmonary artery smooth muscle cells: role of pro-inflammatory cytokines. *Am J Physiol Lung Cell Mol Physiol* 302:L604–L615
6. Dewachter L, Adnot S, Guignabert C, Tu L, Marcos E, Fadel E, Humbert M, Dartevielle P, Simonneau G, Naeije R, Eddahibi S (2009) Bone morphogenetic protein signalling in heritable versus idiopathic pulmonary hypertension. *Eur Respir J* 34:1100–1110
7. Dorfmueller P, Humbert M, Perros F, Sanchez O, Simonneau G, Muller KM, Capron F (2007) Fibrous remodeling of the pulmonary venous system in pulmonary arterial hypertension associated with connective tissue diseases. *Hum Pathol* 38:893–902
8. Eddahibi S, Guignabert C, Barlier-Mur AM, Dewachter L, Fadel E, Dartevielle P, Humbert M, Simonneau G, Hanoun N, Saurini F, Hamon M, Adnot S (2006) Cross talk between endothelial and smooth muscle cells in pulmonary hypertension: critical role for serotonin-induced smooth muscle hyperplasia. *Circulation* 113:1857–1864
9. Elliott CG, Glissmeyer EW, Havlena GT, Carlquist J, McKinney JT, Rich S, McGoan MD, Scholand MB, Kim M, Jensen RL, Schmidt JW, Ward K (2006) Relationship of *BMPR2* mutations to vasoreactivity in pulmonary arterial hypertension. *Circulation* 113:2509–2515
10. Hassoun PM, Mouthon L, Barbera JA, Eddahibi S, Flores SC, Grimminger F, Jones PL, Maitland ML, Michelakis ED, Morrell NW, Newman JH, Rabinovitch M, Schemmuly R, Stenmark KR, Voelkel NF, Yuan JX, Humbert M (2009) Inflammation, growth factors, and pulmonary vascular remodeling. *J Am Coll Cardiol* 54:S10–S19
11. Heresi GA, Aytakin M, Hammel JP, Wang S, Chatterjee S, Dweik RA (2014) Plasma interleukin-6 adds prognostic information in pulmonary arterial hypertension. *Eur Respir J* 43:912
12. Hong KH, Lee YJ, Lee E, Park SO, Han C, Beppu H, Li E, Raizada MK, Bloch KD, Oh SP (2008) Genetic ablation of the *BMPR2* gene in pulmonary endothelium is sufficient to predispose to pulmonary arterial hypertension. *Circulation* 118:722–730
13. Huertas A, Perros F, Tu L, Cohen-Kaminsky S, Montani D, Dorfmueller P, Guignabert C, Humbert M (2014) Immune dysregulation and endothelial dysfunction in pulmonary arterial hypertension: a complex interplay. *Circulation* 129:1332–1340
14. Humbert M, Monti G, Brenot F, Sitbon O, Portier A, Grangeot-Keros L, Duroux P, Galanaud P, Simonneau G, Emilie D (1995) Increased interleukin-1 and interleukin-6 serum concentrations in severe primary pulmonary hypertension. *Am J Respir Crit Care Med* 151:1628–1631
15. Humbert M, Morrell NW, Archer SL, Stenmark KR, MacLean MR, Lang IM, Christman BW, Weir EK, Eickelberg O, Voelkel NF, Rabinovitch M (2004) Cellular and molecular pathobiology of pulmonary arterial hypertension. *J Am Coll Cardiol* 43:13S–24S
16. Kim CW, Song H, Kumar S, Nam D, Kwon HS, Chang KH, Son DJ, Kang DW, Brodie SA, Weiss D, Vega JD, Alberts-Grill N, Griendling K, Taylor WR, Jo H (2013) Anti-inflammatory and antiatherogenic role of BMP receptor II in endothelial cells. *Arterioscler Thromb Vasc Biol* 33:1350–1359
17. LaRaia AV, Waxman AB (2007) Pulmonary arterial hypertension: evaluation and management. *South Med J* 100:393–399
18. Li M, Vattulainen S, Aho J, Orcholowski M, Rojas V, Yuan K, Helenius M, Taimen P, Myllykangas S, De Jesus Perez V, Koskenvuo JW, Alastalo TP (2014) Loss of bone morphogenetic protein receptor 2 is associated with abnormal DNA repair in pulmonary arterial hypertension. *Am J Respir Cell Mol Biol* 50:1118–1128
19. Long L, MacLean MR, Jeffery TK, Morecroft I, Yang X, Rudarakanchana N, Southwood M, James V, Trembath RC, Morrell NW (2006) Serotonin increases susceptibility to pulmonary hypertension in *BMPR2*-deficient mice. *Circ Res* 98:818–827
20. Machado RD, Aldred MA, James V, Harrison RE, Patel B, Schwalbe EC, Gruenig E, Janssen B, Koehler R, Seeger W, Eickelberg O, Olschewski H, Elliott CG, Glissmeyer E, Carlquist J, Kim M, Torbicki A, Fijalkowska A, Szweczyk G, Parma J, Abramowicz MJ, Galie N, Morisaki H, Kyotani S, Nakanishi N, Morisaki T, Humbert M, Simonneau G, Sitbon O, Soubrier F,

- Coulet F, Morrell NW, Trembath RC (2006) Mutations of the TGF-beta type II receptor BMPR2 in pulmonary arterial hypertension. *Hum Mutat* 27:121–132
21. Machado RD, Eickelberg O, Elliott CG, Geraci MW, Hanaoka M, Loyd JE, Newman JH, Phillips JA III, Soubrier F, Trembath RC, Chung WK (2009) Genetics and genomics of pulmonary arterial hypertension. *J Am Coll Cardiol* 54:S32–S42
  22. Massague J (2012) TGFbeta signalling in context. *Nat Rev Mol Cell Biol* 13:616–630
  23. McLaughlin VV, McGoon MD (2006) Pulmonary arterial hypertension. *Circulation* 114:1417–1431
  24. Miyazono K, Maeda S, Imamura T (2005) BMP receptor signaling: transcriptional targets, regulation of signals, and signaling cross-talk. *Cytokine Growth Factor Rev* 16:251–263
  25. Morrell NW, Adnot S, Archer SL, Dupuis J, Jones PL, MacLean MR, McMurtry IF, Stenmark KR, Thistlethwaite PA, Weissmann N, Yuan JX, Weir EK (2009) Cellular and molecular basis of pulmonary arterial hypertension. *J Am Coll Cardiol* 54:S20–S31
  26. Morrell NW, Yang X, Upton PD, Jourdan KB, Morgan N, Sheares KK, Trembath RC (2001) Altered growth responses of pulmonary artery smooth muscle cells from patients with primary pulmonary hypertension to transforming growth factor-beta(1) and bone morphogenetic proteins. *Circulation* 104:790–795
  27. Newman JH, Trembath RC, Morse JA, Grunig E, Loyd JE, Adnot S, Coccolo F, Ventura C, Phillips JA III, Knowles JA, Janssen B, Eickelberg O, Eddahibi S, Herve P, Nichols WC, Elliott G (2004) Genetic basis of pulmonary arterial hypertension: current understanding and future directions. *J Am Coll Cardiol* 43:33S–39S
  28. Pfarr N, Szamalek-Hoegel J, Fischer C, Hinderhofer K, Nagel C, Ehlken N, Tiede H, Olschewski H, Reichenberger F, Ghofrani AH, Seeger W, Grunig E (2011) Hemodynamic and clinical onset in patients with hereditary pulmonary arterial hypertension and BMPR2 mutations. *Respir Res* 12:99
  29. Prewitt AR, Ghose S, Frump AL, Datta A, Austin ED, Kenworthy AK, de Caestecker MP (2015) Heterozygous null bone morphogenetic protein receptor type 2 mutations promote SRC kinase-dependent caveolar trafficking defects and endothelial dysfunction in pulmonary arterial hypertension. *J Biol Chem* 290:960–971
  30. Pullamsetti SS, Schermuly R, Ghofrani A, Weissmann N, Grimminger F, Seeger W (2014) Novel and emerging therapies for pulmonary hypertension. *Am J Respir Crit Care Med* 189:394–400
  31. Quarck R, Nawrot T, Meyns B, Delcroix M (2009) C-reactive protein: a new predictor of adverse outcome in pulmonary arterial hypertension. *J Am Coll Cardiol* 53:1211–1218
  32. Quarck R, Wynants M, Ronisz A, Sepulveda MR, Wuytack F, Van RD, Meyns B, Delcroix M (2012) Characterization of proximal pulmonary arterial cells from chronic thromboembolic pulmonary hypertension patients. *Respir Res* 13:27
  33. Rabinovitch M, Guignabert C, Humbert M, Nicolls MR (2014) Inflammation and immunity in the pathogenesis of pulmonary arterial hypertension. *Circ Res* 115:165–175
  34. Ranchoux B, Antigny F, Rucker-Martin C, Hautefort A, Pechoux C, Bogaard HJ, Dorfmueller P, Remy S, Lecerf F, Plante S, Chat S, Fadel E, Houssaini A, Anegon I, Adnot S, Simonneau G, Humbert M, Cohen-Kaminsky S and Perros F (2015) Endothelial-to-Mesenchymal Transition in Pulmonary Hypertension. *Circulation*
  35. Rosenzweig EB, Morse JH, Knowles JA, Chada KK, Khan AM, Roberts KE, McElroy JJ, Juskiw NK, Mallory NC, Rich S, Diamond B, Barst RJ (2008) Clinical implications of determining BMPR2 mutation status in a large cohort of children and adults with pulmonary arterial hypertension. *J Heart Lung Transplant* 27:668–674
  36. Ross DJ, Strieter RM, Fishbein MC, Ardehali A, Belperio JA (2012) Type I immune response cytokine-chemokine cascade is associated with pulmonary arterial hypertension. *J Heart Lung Transplant* 31:865–873
  37. Sawada H, Saito T, Nickel NP, Alastalo TP, Glotzbach JP, Chan R, Haghighat L, Fuchs G, Januszynski M, Cao A, Lai YJ, Perez VJ, Kim YM, Wang L, Chen PI, Spiekeroetter E, Mitani Y, Gurtner GC, Sarnow P, Rabinovitch M (2014) Reduced BMPR2 expression induces GM-CSF translation and macrophage recruitment in humans and mice to exacerbate pulmonary hypertension. *J Exp Med* 211:263–280
  38. Simonneau G, Gatzoulis MA, Adatia I, Celermajer D, Denton C, Ghofrani A, Gomez Sanchez MA, Krishna KR, Landzberg M, Machado RF, Olschewski H, Robbins IM, Souza R (2013) Updated clinical classification of pulmonary hypertension. *J Am Coll Cardiol* 62:D34–D41
  39. Song Y, Jones JE, Beppu H, Keaney JF Jr, Loscalzo J, Zhang YY (2005) Increased susceptibility to pulmonary hypertension in heterozygous BMPR2-mutant mice. *Circulation* 112:553–562
  40. Soon E, Holmes AM, Treacy CM, Doughty NJ, Southgate L, Machado RD, Trembath RC, Jennings S, Barker L, Nicklin P, Walker C, Budd DC, Pepke-Zaba J, Morrell NW (2010) Elevated levels of inflammatory cytokines predict survival in idiopathic and familial pulmonary arterial hypertension. *Circulation* 122:920–927
  41. Soon E, Crosby A, Southwood M, Yang P, Tajsic T, Toshner M, Appleby S, Shanahan CM, Bloch KD, Pepke-Zaba J, Upton P, Morrell NW (2015) Bone morphogenetic protein receptor type II deficiency and increased inflammatory cytokine production. A gateway to pulmonary arterial hypertension. *Am J Respir Crit Care Med* 192:859–872
  42. Soubrier F, Chung WK, Machado R, Grunig E, Aldred M, Geraci M, Loyd JE, Elliott CG, Trembath RC, Newman JH, Humbert M (2013) Genetics and genomics of pulmonary arterial hypertension. *J Am Coll Cardiol* 62:D13–D21
  43. Stacher E, Graham BB, Hunt JM, Gandjeva A, Groshong SD, McLaughlin VV, Jessup M, Grizzle WE, Aldred MA, Cool CD, Tuder RM (2012) Modern age pathology of pulmonary arterial hypertension. *Am J Respir Crit Care Med* 186:261–272
  44. Star GP, Giovinazzo M, Langleben D (2013) ALK2 and BMPR2 knockdown and endothelin-1 production by pulmonary microvascular endothelial cells. *Microvasc Res* 85:46–53
  45. Upton PD, Morrell NW (2013) The transforming growth factor-beta bone morphogenetic protein type signalling pathway in pulmonary vascular homeostasis and disease. *Exp Physiol* 98:1262–1266
  46. Wang H, Ji R, Meng J, Cui Q, Zou W, Li L, Wang G, Sun L, Li Z, Huo L, Fan Y, Penny DJ (2014) Functional changes in pulmonary arterial endothelial cells associated with BMPR2 mutations. *PLoS One* 9:e106703
  47. Wynants M, Quarck R, Ronisz A, Alfaro-Moreno E, Van RD, Meyns B, Delcroix M (2012) Effects of C-reactive protein on human pulmonary vascular cells in chronic thromboembolic pulmonary hypertension. *Eur Respir J* 40:886–894